Accepted Manuscript

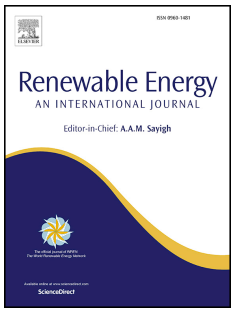

Degradation issues of PEM electrolysis MEAs

S. Siracusano, N. Van Dijk, R. Backhouse, L. Merlo, V. Baglio, A.S. Arico

PII: S0960-1481(18)30167-8

DOI: 10.1016/j.renene.2018.02.024

Reference: RENE 9755

To appear in: *Renewable Energy*

Received Date: 30 October 2017

Revised Date: 9 January 2018

Accepted Date: 4 February 2018

Please cite this article as: Siracusano S, Van Dijk N, Backhouse R, Merlo L, Baglio V, Arico AS, Degradation issues of PEM electrolysis MEAs, *Renewable Energy* (2018), doi: 10.1016/j.renene.2018.02.024.

Degradation issues of PEM electrolysis MEAs

S. Siracusano[1*], N. Van Dijk[2], R. Backhouse[2], L. Merlo[3], V. Baglio[1], A. S. Arico[1]

[1] *CNR-ITAE, Via Salita S. Lucia sopra Contesse 5 – 98126 Messina, Italy*

[2] *ITM Power (Research) Ltd, Unit H, Sheffield Airport Business Park, Europa Link, Sheffield S9 1XU*

[3] *Solvay Specialty Polymers Italy SpA, viale Lombardia, 20 20021 – Bollate, Italy*

Abstract

One of main challenge of proton exchange membrane (PEM) water electrolysis is the achievement of a long-term durability exceeding 100 khours. Accordingly, degradation mechanisms of membrane electrode assemblies (MEAs) and stack components of PEM electrolysers deserve large attention. An important objective of the EU ELECTROHYPEM project was to develop components for PEM electrolysers with enhanced activity and stability in order to reduce stack and system costs and to improve efficiency, performance and durability. The focus of the project was concerning mainly with electrocatalysts and membranes development and validation of these materials in a PEM electrolyser. In this work, a first set of MEAs, used for 3500-5700 hours in a PEM electrolyser, was investigated using electrochemical and physico-chemical techniques. The goal was to individuate key degradation issues and to provide a reliable estimation of the MEA endurance under real life operation. Specific approaches to mitigate the degradation mechanisms are discussed.

Keywords: PEM Water electrolysis; Degradation Mechanisms; Iridium-ruthenium oxide electrocatalyst; perfluoro-sulfonic membranes; Pt electrocatalysts.

1. Introduction

Sustainable hydrogen production can meet an increasing share of the hydrogen demand for energy applications from carbon-free or lean energy sources. Water electrolysis appears as one of the most practical technologies used to produce hydrogen from renewable energy sources (RES) [1-4].

It is widely accepted that the operating expenditures of a PEM electrolysis system are strongly related to the endurance characteristics [5-7]. These are significantly affected by the MEA durability [8-11]. The stability characteristics of electrolysis cells have been widely investigated in the literature and relevant degradation mechanisms have been identified [12-20]. These mechanisms are especially correlated with the materials properties, operating conditions, but also with the shaping of the materials and the setting up of the MEAs in the stack [19]. However, specific attention should be also deserved to the MEA manufacturing. Our evidence is that there is a paramount effect of the MEA production procedure on the endurance characteristics [21, 22]. In particular, the optimization of specific manufacturing parameters appears to affect significantly the durability of the MEA.

In general, the fabrication procedure of the MEA plays a vital role in determining the performance, production costs and longevity of the electrolyser. One of the methods frequently used for water electrolysis MEA fabrication is the catalyst coated membrane (CCM) technique [1, 21, 22]. The catalyst is mixed with ionomer in an appropriate solvent and dispersed under sonification; the corresponding ink is then deposited onto the membrane typically by direct spraying or by decal transfer [1, 21, 23, 24]. Spraying techniques are preferred as they can be automated and thus are more amenable to productionisation. In these methods, significant effort is focused on extending the triple-phase boundary by proper dispersion of the ionomer in the catalytic layer [25-27]. These procedures are optimised to enhance both electronic and ionic percolations within the catalytic layer. The deposition of a mixed ionic-electronically conducting layer directly onto the membrane increases catalyst utilization and reduces the chances of a junction potential at the catalyst-

membrane interface. Besides enhancing the performance, these procedures serve to optimise the noble metal loadings by increasing catalyst utilization [26, 27].

The basic aspects of air assisted spray coating or ultrasonic spray coating is to feed a low viscosity ink to the spray head with a precision metering pump where the ink is atomized into a fine mist and directed onto the heated polymer membrane. However, a relevant aspect observed in this work is regarding the effect of the post-deposition hot pressing procedure on the stability of the prepared MEAs. Usually, hot pressing is carried out at a temperature above the glass transition temperature of the polymeric membrane. However, the use of high temperature treatments may produce structural changes and modification of the properties of the active components. These aspects are seldom investigated in the literature. The present analysis aims at covering such gaps and to identify relevant degradation mechanisms. In this regard, the performance and stability of various MEAs obtained using the same basic components (i.e. catalysts and membranes) but prepared according to different hot-pressing procedures are reported.

2. Experimental

Physico-chemical and morphological characterizations were carried out for both fresh and used (after 3500 hrs durability test) MEAs.

XRD was performed on the electrode layers by a Philips X-Pert diffractometer equipped with a CuKα as radiation source. This diffractometer was operated at 40 kV and 20 mA, with a scan rate of 0.5 2θ min^{-1} and angular resolution of 0.005° 2θ. The diffraction patterns were fitted to the Joint Committee on Powder Diffraction Standards (JCPDS).

Scanning Electron Microscopy (SEM) with Energy Dispersive X-Ray (EDX) analysis was carried out by a FEI XL30 SFEG microscope. The instrument was operated at 25 kV and the EDX probe was used to determine the bulk elemental composition of the anodes before and after the durability test.

The morphology of the IrRuOx and Pt/C electrodes was investigated by transmission electron microscopy (TEM) using a Philips CM12 instrument. The specimens were prepared by ultrasonic dispersion of the electrode in isopropyl alcohol and subsequently depositing a drop of the suspension on a carbon-coated Cu grid.

MEAs were manufactured in house using Aquivion E098-09 as the membrane and IrRuOx and Pt black as the anode and cathode catalysts, respectively. The anode and cathode catalysts loading was 3 $mg \cdot cm^{-2}$ on both sides. The optimum ink formulation consisted of a 4:1 ratio of catalyst: ionomer in an aqueous solution containing a dispersant to prevent catalyst agglomeration and setting. Typically, both sides of the membrane are sprayed with the relevant catalyst inks then the sprayed membrane is hot-pressed to form a bond between the membrane and the catalyst layer. In particular, this technique shows good results with the fluorinated polymers [22]. In this work, different hot pressing procedures were applied to the MEAs in order to find out the most suitable condition, to achieve higher performance and longer life-time. MEA A and B were laminated at 200°C for 1.5 and 3 min, respectively. MEA C and D were laminated at 180°C for 1.5 and 3 min, respectively. Hot pressed MEAs were assembled into an acrylic lab cell containing Ti plates as current collectors with an active area of 8 cm^2. A standard ITM Power Ltd (UK) electrolysis cell testing set-up made of Ti plates and diffusion layer both at the anode and cathode was used. Electrochemical analysis has been carried out using a power supplier and a frequency response analyser (FRA).

3. Results and discussion

MEAs were run at constant current (1 A/cm^2) and 55°C. Time studies are shown in Fig. 1. Tests lasted 3500 or 5750 hrs in lab scale cells. All samples, regardless of their hot pressing temperature, showed a reversible degradation. MEAs pressed at 200°C, samples A and sample B (pale and orange lines in Fig. 1) showed higher voltage rise than those pressed at 180°C , samples C and sample D (yellow and dark green lines in Fig. 1). Moreover, a prolonged lamination procedure 3

104 min instead of 1.5 min was not beneficial, especially at the highest lamination temperature. Shorter
105 lamination times resulted in a non-appropriate adhesion of the catalytic layer to the membrane.
106 Thus, MEAs hot pressed at 200°C and for longer times appeared to degrade faster than those
107 pressed at 180°C and for shorter times. Starting cell voltages were 1.70 V and 1.71 V for 180°C
108 hot-pressed MEAs at 1 A/cm^2; they went up to approximately 1.73 V in 5700 hrs and gave a decay
109 rate of 3.3 μV/h (Figure 1, a).

110 In this work, specific attention was deserved to the degradation of the MEAs treated at 200°C,
111 which were less stable than those treated at 180°C. Figures 1b and 1c show ac-impedance spectra at
112 55 °C, at open circuit voltage (OCV) and 50, 100, 200 mA/cm^2 for the MEAs hot-pressed for 3 min
113 at 180°C (Fig. 1, b) and 200°C (Fig. 1, c). These were measured at the beginning and after 2600
114 hours of the time-test. The series resistance (R_s) is determined from the high frequency intercept on
115 the X-axis of the Nyquist plot (lowest Z' values). This is associated mainly to the thickness and
116 conductivity of the membrane. The polarization resistance was obtained by the difference between
117 the low (high Z' values) and high frequency (low Z' values) intercepts on the real axis. As
118 expected, there was a progressive decrease of polarization resistance with an increase of the applied
119 current density according to the enhancement in reaction kinetics. However, upon prolonged
120 electrolysis operation, EIS indicates an increase in the polarisation resistance for the same operating
121 current density. Such evidence was more relevant for the sample laminated at 200 °C for 3 min
122 compared to the sample laminated at 180 °C for 3 min. This confirms the faster degradation for the
123 200°C hot-pressed MEA. In principle, a catalyst degradation, a loss of ionomer from the catalyst
124 layer or any other structural changes within the catalytic layer could be the cause of this evidence.
125 In addition, it was evident a decrease of the series resistance upon ageing in both cases but the
126 change in series resistance was larger for the sample laminated at 200 °C than that laminated at
127 180°C. Decrease of series resistance may be indicative of membrane thinning (see below).

128 To better understand the degradation causes, ex-situ post-operation analyses have been carried
129 out on the sample B 200°C, 3 min – laminated MEA, worked for 3500 hours and compared to a

fresh MEA with the same characteristics. XRD patterns of fresh and used anode (a) and fresh and used cathode (b) side MEAs are reported in Figure 2. No dramatic change in crystallite size, for both anode and cathode, in the used samples, was observed. There is an evidence of the X-ray diffraction peaks from both catalytic layer in the used samples due to a membrane thinning effect after the endurance tests as envisaged from SEM analysis (see below). This causes a lower shielding of the incoming X-rays. An increase of ionomer scattering in the XRD patterns of used samples is likely associated to an increased contribution of the X-ray scattering from the membrane.

TEM images of anode and cathode side of fresh and used MEAs are reported in Figure 3. The anode micrographs show the presence of agglomerates composed of fine IrRuOx particles (2-3 nm). In the case of fresh cathode, the unsupported Pt primary particles are of 5-10 nm. Similar particle size and agglomeration features are present in the anode of the used MEA compared to fresh MEA (2-3 nm); whereas, there is a slight particle size increase at the cathode; primary particles show 7-10 nm mean particle size.

In Figure 4, the SEM micrographs (section view) of fresh and used MEAs are reported. No relevant changes in catalytic layer thickness of fresh vs. used MEAs was observed. According to the magnified view in Fig. 4 (bottom), the upper catalytic layer (cathode) thickness decreases from about 13 µm to 12 µm (average); the lower catalytic layer (anode) thickness remains almost constant at 16 µm (average) after the endurance tests. On the contrary, a membrane thinning effect was evident (up to 50%). The effect of cell compression and dehydration under high vacuum (raw and used membranes had a different hydration state) can play a role in causing such polymer shrinkage. However, a decrease of the series resistance was observed in the impedance spectra in Fig. 1 upon ageing. This seems to confirm the membrane thinning even if the observed decrease in R_s accounts for a much lower variation in thickness than 50%.

The EDX comparison of fresh and used anode side of the MEAs is reported in Figure 5. Some Ru dissolution appeared evident (EDX carried out at low magnification analysis) in the used sample. There was also a slight decrease of the F signal compared to Ir in the used sample. This was

a different evidence than that derived from XRD, where an increase of the ionomer peak was observed. Moreover, the presence of Fe and Ti impurities in the used sample was evident.

In the case of the EDX comparison of fresh and used cathode side of the MEAs, reported in Figure 6, a slight decrease of fluorine vs. Pt was observed, but there was no evidence of impurities. Ionomer and membrane degradation in the set of MEAs here analysed could be affected by the high temperature MEA fabrication (200°C) in this case. This could have caused a chemical degradation of non stabilised ionomer and membrane during the manufacturing procedure.

From the above analysis, the main sources of degradation for this first set of MEAs (A-D) were individuated and reported below in order of relevance: 1) Presence of impurities of Fe from the cell testing set-up: these species affect ionic conductivity and accelerate membrane/ionomer degradation. Fe contamination probably comes from the stainless steel pipelines of the test station. Corrosion of stainless steel pipelines may be exacerbated by the release of hydrofluoric acid from the membrane/ionomer degradation during operation. 2) Ru dissolution from the nanosized IrRuOx catalyst: probably, the fraction of Ru that is less alloyed, or non-alloyed to Ir, dissolves under operating conditions. 3) Ti plate degradation at the cathode side is another relevant source of performance decay and could be related to the release of fluoride species. Titanium plates and diffusion layers are conventionally used in Proton Exchange Membrane Water Electrolysis both at the anode and cathode. The thin oxide film usually present on titanium outermost surface layers is very stable and is only attacked by a few substances, most notably, hydrofluoric acid (HF). As well known, degradation of the perfluorosulfonic ionomers can give rise to hydrofluoric acid. A slight change in colour at the cathode plate would indicate some attack possibly related to HF release .4) Ionomer content decreases, and, possibly, it gives rise to restructuring. 5) Membrane thinning and changes in the catalyst-membrane interface also occur and may affect hydrogen cross-over.

The approaches used to mitigate the degradation mechanisms for the Electrohypem second set of MEAs were: *i)* a pre-leaching procedure in perchloric acid to remove all impurities due to the synthesis of electrocatalysts [28]; *ii)* the degree of alloying in the mixed oxide catalysts was

improved through a specific thermal treatment and particle size increased to 5-10 nm [28]; *iii)* to allow for better stability the unsupported Pt cathode catalyst was replaced with a carbon supported (Pt/C) cathode catalyst with large surface area [29]; *iv)* a chemical stabilisation of membrane and ionomer was carried out in order to avoid the release of fluorine species. The stabilization process for the membrane/ionomer consists in a post-fluorination treatment of the polymer powder to convert some defects, in particular terminal carboxylic groups, into C-F groups before the polymer extrusion process. [21, 29]; *v)* the development of a specific coating for Ti plates was adopted. A stack based on such advanced components was demonstrated in the Electrohypem Project [30] providing very good performance and stability.

PEM electrolysis MEA degradation mechanisms have been recently reviewed in the literature [31, 32]. Main evidences regard dissolution of catalysts, ionomer dissolution, cation contamination, chemical degradation, hydrogen embrittlement, passivation, mechanical degradation and involve catalytic layers, membrane, bipolar plate and current collectors [31]. High fluorides content from conventional Nafion 117 perfluorosulfonic acid membrane degradation was especially found on the cathode side [32].

We have essentially observed similar evidences especially in our first set of non optimised MEAs. This means that such problems are common to different materials and MEA systems. Accordingly, the discussed mitigation strategies can be of general interest.

4. Conclusion

The effect of the hot pressing treatment on the MEA fabrication procedures was investigated in this work. The hot pressed CCM route seems to give rise to both good performance and reproducibility. However, specific optimization of the hot pressing procedure is required for productionisation. This affects significantly performance and stability. Mitigation strategies to reduce MEA degradation have been discussed. Optimised MEAs have provided excellent stability with very low irreversible decay (<3 μV/h) in tests exceeding 5000 hrs at 55°C. However, there was still some relevant

reversible degradation, not necessarily associated to the CCM properties, but possibly to the diffusion layer characteristics.

Acknowledgement

The authors acknowledge the financial support of the EU through the FCH JU Electrohypem Project. “The research leading to these results has received funding from the European Community's Seventh Framework Programme (FP7/2010-2013) for the Fuel Cells and Hydrogen Joint Technology Initiative under grant agreement Electrohypem n° 300081.”

References

[1] M. Carmo, D.L. Fritz, J. Mergel, D. Stolten, A comprehensive review on PEM water electrolysis, Int. J. Hydrogen Energy 38 (2013) 4901-4934.

[2] A.S. Aricò, S. Siracusano, N. Briguglio, V. Baglio, A. Di Blasi, V. Antonucci, Polymer electrolyte membrane water electrolysis: status of technologies and potential applications in combination with renewable power sources, J. Appl. Electrochem. 43 (2013) 107-118.

[3] F. Barbir, PEM electrolysis for production of hydrogen from renewable energy sources, Sol. Energy 78 (2005) 661-669.

[4] S. Mesfun, D.L. Sanchez, S. Leduc, E. Wetterlund, J. Lundgren, M. Biberacher, F. Kraxner, Power-to-gas and power-to-liquid for managing renewable electricity intermittency in the Alpine Region Renewable Energy 107 (2017) 361-372.

[5] A. Marshall, B. Børresen, G. Hagen, M. Tsypkin, R. Tunold, Hydrogen production by advanced proton exchange membrane (PEM) water electrolysers. Energy 32 (2007) 431-436.

[6] S. Siracusano, A. Di Blasi, V. Baglio, G. Brunaccini, N. Briguglio, A. Stassi, R. Ornelas, E. Trifoni, V. Antonucci, A.S. Aricò, Optimization of components and assembling in a PEM electrolyzer stack Int. J. Hydrogen Energy 36 (2011) 3333-3339.

[7] M. Götz, J. Lefebvre, F. Mörs, A. McDaniel Koch, F. Graf, S. Bajohr, R. Reimert, T. Kolb, Renewable Power-to-Gas: A technological and economic review. Renewable Energy 85 (2016) 1371-1390.

[8] F. Andolfatto, R. Durand, A. Michas, P. Millet, P. Stevens, Solid polymer electrolyte water electrolysis: electrocatalysis and long-term stability. Int. J. Hydrogen Energy 19 (1994) 421-427.

[9] P. Millet, R. Ngameni, S.A. Grigoriev, N. Mbemba, F. Brisset, A. Ranjbari, Etiévant C. PEM water electrolyzers: From electrocatalysis to stack development. Int. J. Hydrogen Energy 35 (2010) 5043-5052.

[10] S. Siracusano, V. Baglio, A. Stassi, R. Ornelas, V. Antonucci, A.S. Aricò, Investigation of IrO_2 electrocatalysts prepared by a sulfite-couplex route for the O_2 evolution reaction in solid polymer electrolyte water electrolyzers. Int. J. Hydrogen Energy 36 (2011) 7822-7831.

[11] P. Millet, N. Mbemba, S.A. Grigoriev, V.N. Fateev, A. Aukauloo, C. Etiévant, Electrochemical performances of PEM water electrolysis cells and perspectives, Int. J. Hydrogen Energy 36 (2011) 4134-4142.

[12] S. Siracusano, V. Baglio, C. D'Urso, V. Antonucci, A.S. Aricò, Preparation and characterization of titanium suboxides as conductive supports of IrO_2 electrocatalysts for application in SPE electrolysers. Electrochim. Acta 54 (2009) 6292-6299.

[13] E. Antolini, Iridium As Catalyst and Cocatalyst for Oxygen Evolution/Reduction in Acidic Polymer Electrolyte Membrane Electrolyzers and Fuel Cells, ACS Catal. 4 (2014) 1426-1440.

[14] Y. Jiao, Y. Zheng, M. Jaroniec, S.Z. Qiao, Design of electrocatalysts for oxygen- and hydrogen-involving energy conversion reactions. Chem. Soc. Rev. 44 (2015) 2060-2086.

[15] R. Gao, H. Zhang, D. Yan, Iron diselenide nanoplatelets: Stable and efficient water-electrolysis catalysts. Nano Energy 31 (2017) 90-95.

[16] S. Siracusano, V. Baglio, S.A. Grigoriev, L. Merlo, V.N. Fateev, A.S. Aricò, The Influence of Iridium Chemical Oxidation State on the Performance and Durability of Oxygen Evolution Catalysts in PEM Electrolysis. J. Power Sources 366 (2017) 105-114.

[17] S. Cherevko, S. Geiger, O. Kasian, N. Kulyk, J.-P. Grote, A. Savan, B.R. Shrestha, S. Merzlikin, B. Breitbach, A. Ludwig, K.J. Mayrhofer, Oxygen and hydrogen evolution reactions on Ru, RuO_2, Ir, and IrO_2 thin film electrodes in acidic and alkaline electrolytes: A comparative study on activity and stability Catal. Today 262 (2016) 170-180.

[18] H.N. Nong, H.-S. Oh, T. Reier, E. Willinger, M.-G. Willinger, V. Petkov, D. Teschner, P. Strasser, Oxide-supported IrNiOx core-shell particles as efficient, cost-effective, and stable catalysts for electrochemical water splitting. Angew. Chem. Int. Ed. Engl. 54 (2015) 2975-2979.

[19] S. Siracusano, N. Hodnik, P. Jovanovic, F. Ruiz-Zepeda, M. Šala, V. Baglio, A.S. Aricò, New insights into the stability of a high performance nanostructured catalyst for sustainable water electrolysis. Nano Energy 40 (2017) 618-632.

[20] I. Katsounaros, S. Cherevko, A. R. Zeradjanin, K.J. J. Mayrhofer, Oxygen electrochemistry as a cornerstone for sustainable energy conversion. Angew. Chem. Int. Ed. 53 (2014) 102-121.

[21] S. Siracusano, V. Baglio, A. Stassi, L. Merlo, E. Moukheiber, A.S.Arico, Performance analysis of short-side-chain Aquivions perfluorosulfonic acid polymer for proton exchange membrane water electrolysis. J. Membrane Science 466 (2014) 1-7.

[22] S. Siracusano, V. Baglio, E. Moukheiber, L. Merlo, A.S. Arico, Performance of a PEM water electrolyser combining an IrRu-oxide anode electrocatalyst and a short-side chain Aquivion membrane. Int. J. Hydrogen Energy 40 (2015) 14430-14435.

[23] Y. Shi, Z. Lu, L. Guo, C. Yan, Fabrication of membrane electrode assemblies by direct spray catalyst on water swollen Nafion membrane for PEM water electrolysis Int. J. Hydrogen Energy 42 (2017) 26183-26191.

[24] Y. Zhang, C. Wang, N. Wan, Z. Liu, Z. Mao, Study on a novel manufacturing process of membrane electrode assemblies for solid polymer electrolyte water electrolysis Electrochem. Commun. 9 (2007) 667-670

[25] M. Prasanna, E.A. Cho, T.H. Lim, I.H. Oh, Effects of MEA fabrication method on durability of polymer electrolyte membrane fuel cells Electrochim. Acta 53 (2008) 5434-5441.

[26] D. Lee, S. Hwang, Effect of loading and distributions of Nafion ionomer in the catalyst layer for PEMFCs Int. J. Hydrogen Energy 33 (2008) 2790-2794.

[27] C.-M. Lai, J.-C. Lin, F.-P. Ting, S.-D. Chyou, K.-L. Hsueh, Contribution of Nafion loading to the activity of catalysts and the performance of PEMFC. Int. J. Hydrogen Energy 33 (2008) 4132-4137.

[28] S. Siracusano, N. Van Dijk, E. Payne-Johnson, V. Baglio, A.S. Aricò, Nanosized IrO_x and $IrRuO_x$ electrocatalysts for the O_2 evolution reaction in PEM water electrolysers. Applied Catalysis B: Environmental 164 (2015) 488-495.

[29] S. Siracusano, V. Baglio, N. Van Dijk, L. Merlo, A.S. Aricò, Enhanced performance and durability of low catalyst loading PEM water electrolyser based on a short-side chain perfluorosulfonic ionomer. Applied Energy 192 (2017) 477-489.

[30] http://cordis.europa.eu/result/rcn/177488_en.html

[31] Q. Feng, X.-Z. Yuan, G. Liu, B. Wei, Z. Zhang, H. Li, H. Wang, A review of proton exchange membrane water electrolysis on degradation mechanisms and mitigation strategies Journal of Power Sources 366 (2017) 33-55.

[32] F. Fouda-Onana, M. Chandesris, V. Médeau, S. Chelghoum, D. Thoby, N. Guillet, Investigation on the degradation of MEAs for PEM water electrolysers part I: Effects of testing conditions on MEA performances and membrane properties, Int. J. Hydrogen Energy, 41 (38), (2016) 16627-16636.

Captions to figures

Figure 1. Durability tests at 1 $A \cdot cm^{-2}$ and 55 °C for differently laminated MEAs in the water electrolysis cell (a); Ac-impedance spectra at 55 °C and 50, 100, 200 mA/cm^2 and OCV for 180°C, 3 min pressed MEA (b); Ac-impedance spectra at 55 °C and 50, 100, 200 mA/cm^2 and OCV for 200°C, 3 min pressed MEA (c).

Figure 2. XRD patterns of Fresh and Used Anode (a) and Fresh and Used Cathode (b) side MEA.

Figure 3. TEM Images of Anode (Fresh (a) and Used (b)) and cathode (Fresh (c) and Used (d)) side of MEAs.

Figure 4. SEM cross section view of 1A new MEA and 1B used MEA.

Figure 5. SEM-EDX front view of fresh and used MEAs (anode side).

Figure 6. SEM-EDX front view of 1A new MEA and 1B used MEA (cathode side).

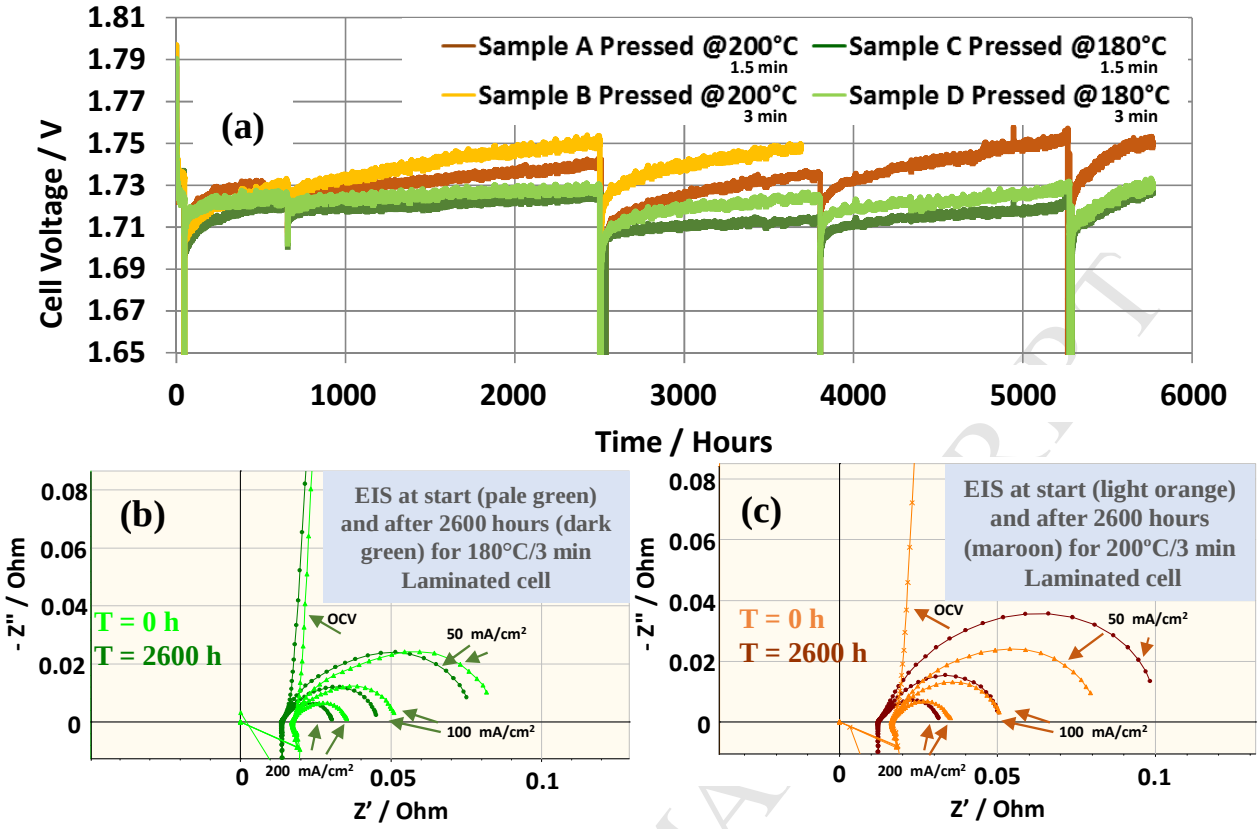

Figure 1

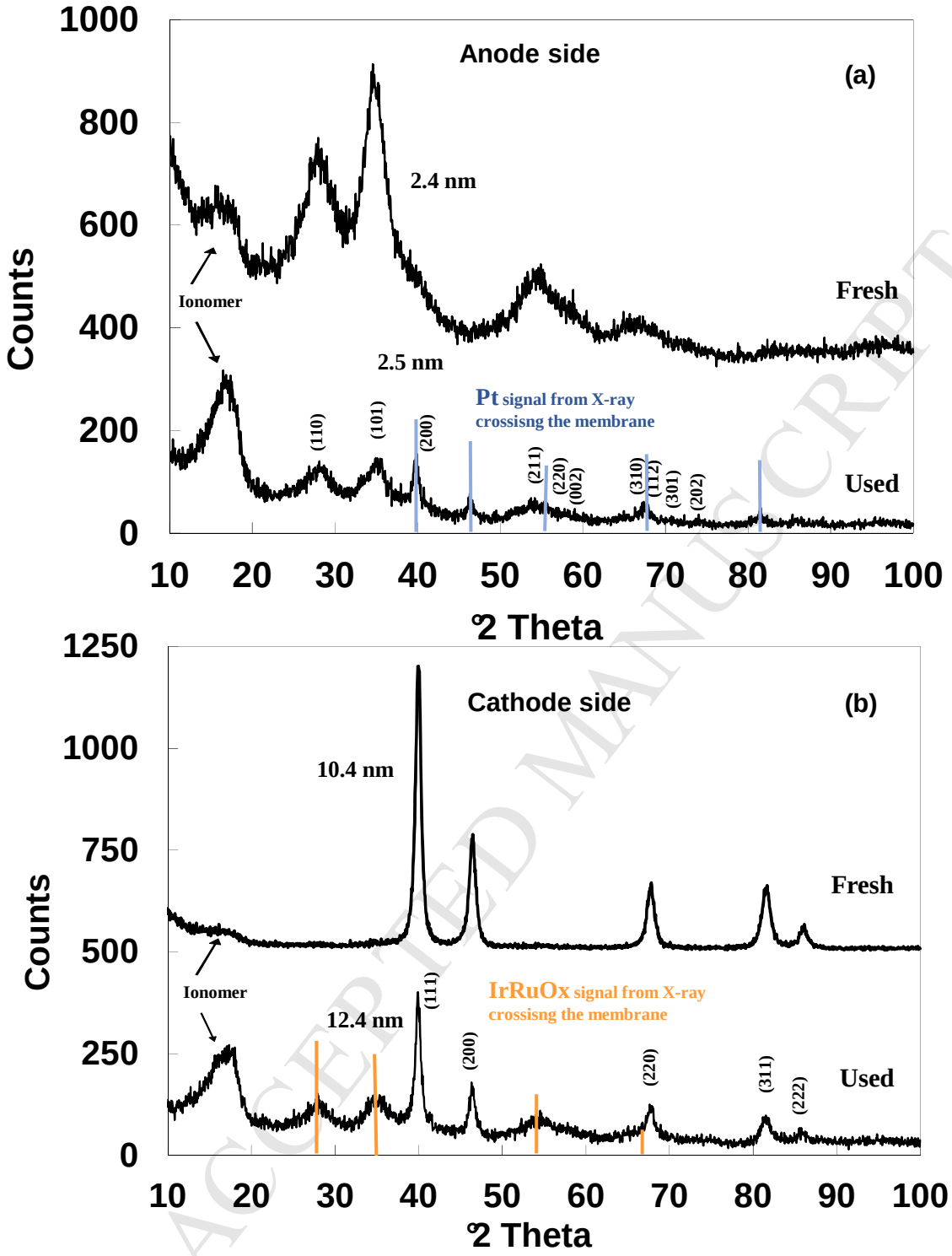

Figure 2

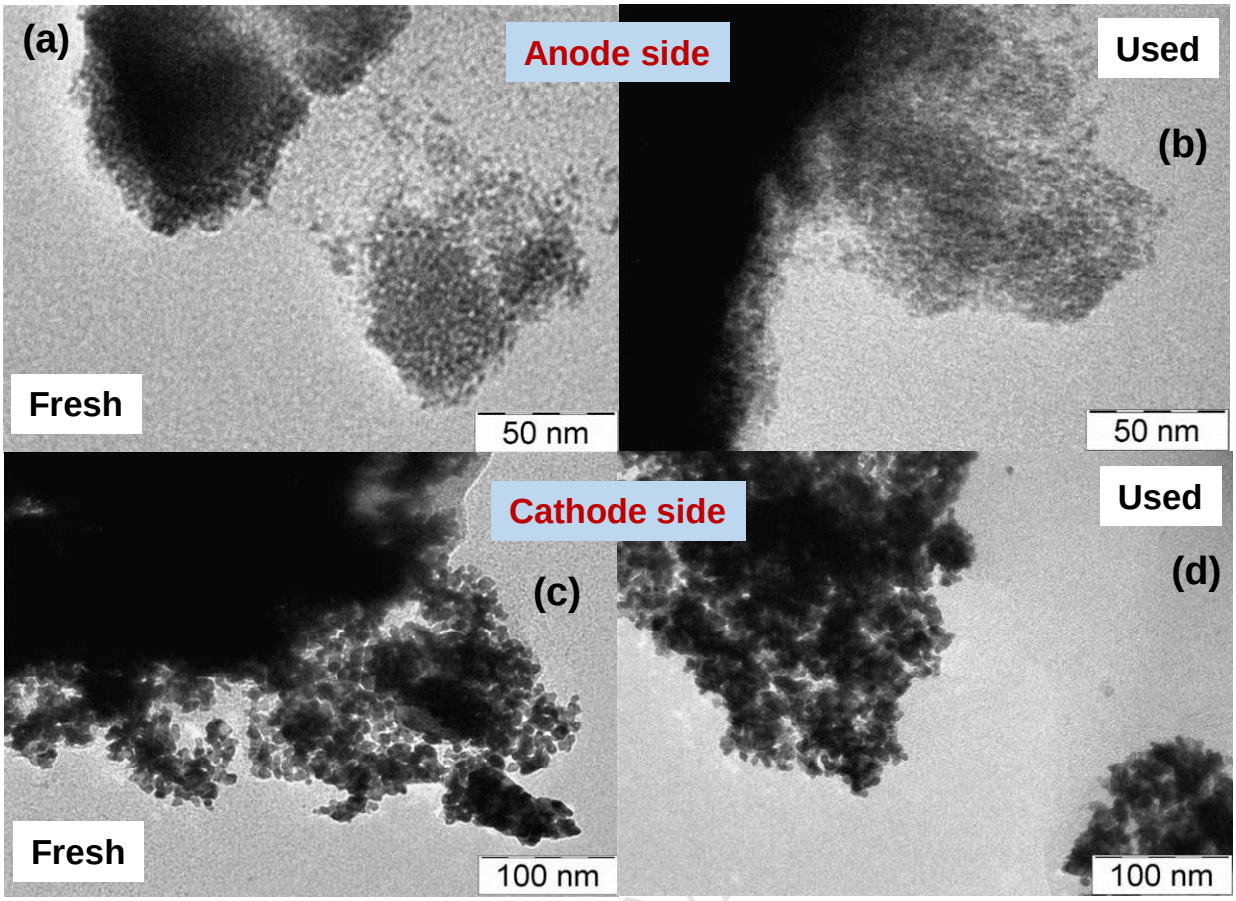

Figure 3

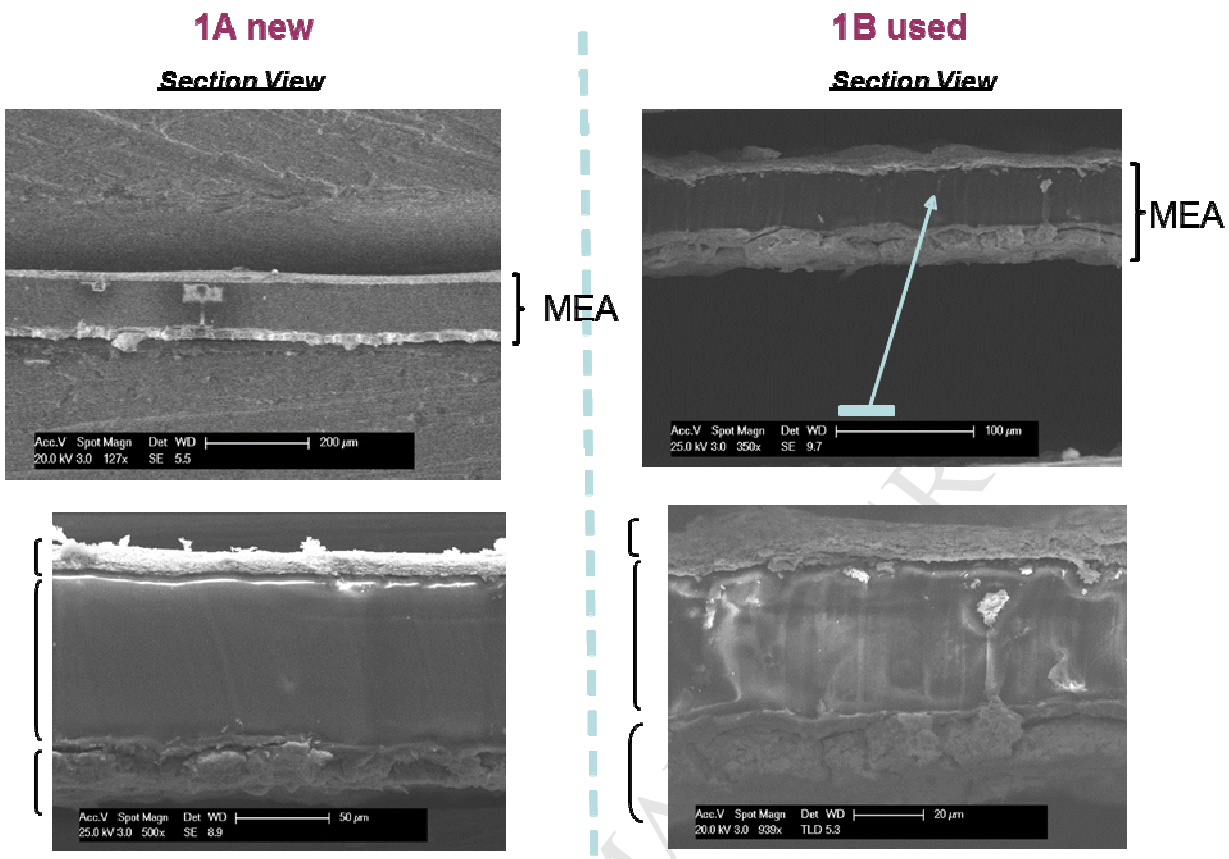

Figure 4

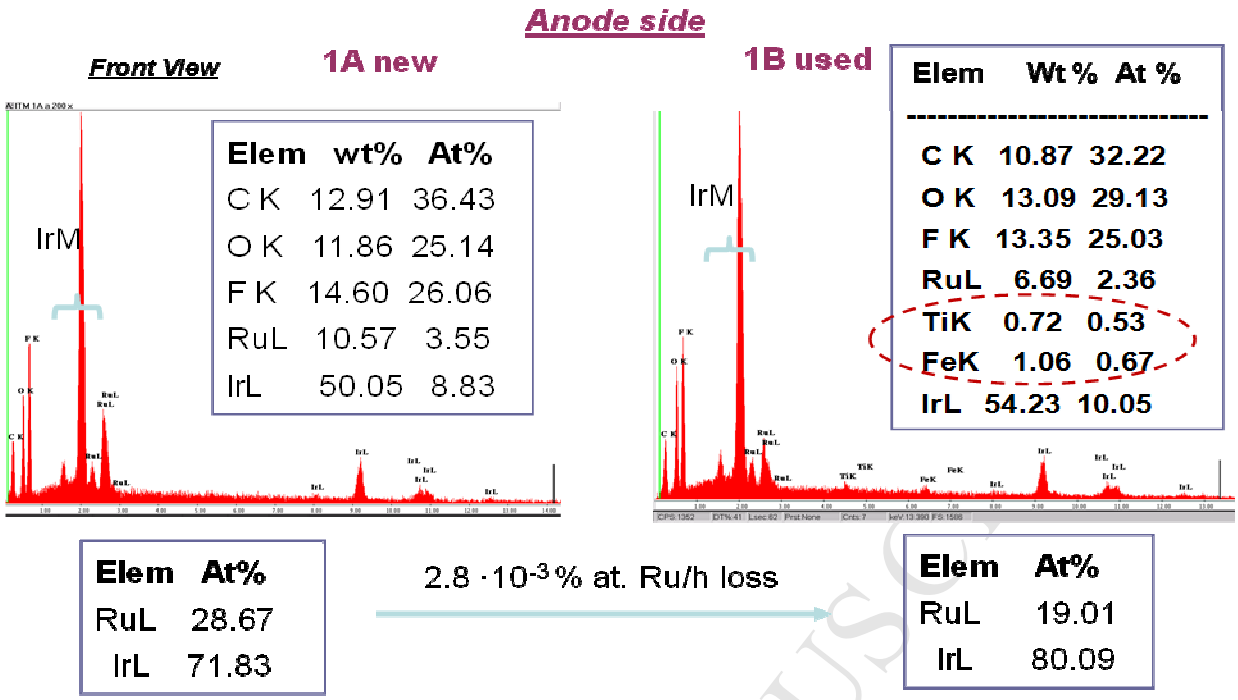

Figure 5

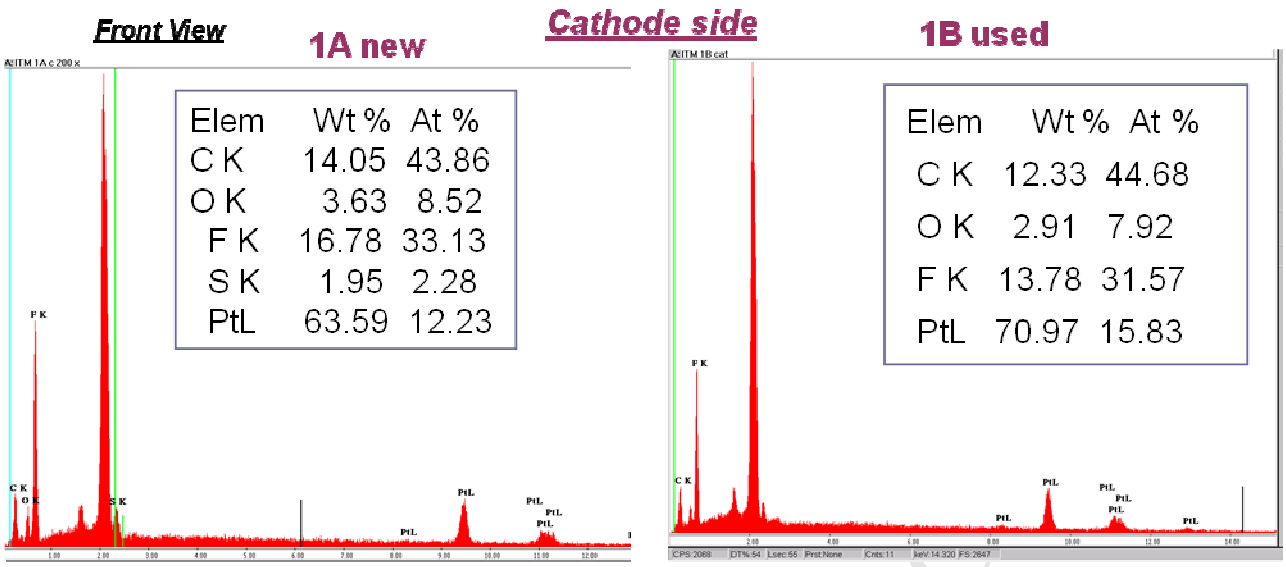

Figure 6